Predicting the replication fidelity of injection molded solid polymer microneedles

Peer-reviewed author version

EVENS, Tim; Castagne, Sylvie; Seveno, David & VAN BAEL, Albert (2022)
Predicting the replication fidelity of injection molded solid polymer microneedles. In:
INTERNATIONAL POLYMER PROCESSING, 37 (3) , p. 237-254.

DOI: 10.1515/ipp-2021-4207
Handle: http://hdl.handle.net/1942/37374

Predicting the replication fidelity of injection moulded solid polymer microneedles

Tim Evens[1], Sylvie Castagne[2], David Seveno[3], Albert Van Bael[1,3]

[1] KU Leuven, Department of Materials Engineering Diepenbeek Campus, Wetenschapspark 27, 3590 Diepenbeek, Belgium

[2] KU Leuven, Department of Mechanical Engineering and Flanders Make@KU Leuven-MaPS, Celestijnenlaan 300, 3001 Leuven, Belgium

[3] KU Leuven, Department of Materials Engineering, Kasteelpark Arenberg 44, 3001 Leuven, Belgium

Correspondence to: Tim Evens (E-mail: tim.evens@kuleuven.be)

ABSTRACT

Microneedles are sharp microscopic features, which can be used for drug or vaccine delivery in a minimally invasive way. Recently, we developed a method to produce polymer microneedles using laser ablated moulds in an injection moulding process. At this moment, extensive injection moulding experiments are needed to investigate the replication fidelity. Accurate predictions of the injection moulding process would eliminate these costly and time expensive experiments. In this study, we evaluated the replication fidelity of solid polymer microneedles using numerical simulations and compared the results to injection moulding experiments. This study was performed for different sizes of microneedles, different thermoplastics (polypropylene and polycarbonate) and different mould materials (tool steel, copper alloy and aluminium alloy). Moreover, different processing conditions and different locations of the microneedles on the macroscopic part were considered. A good correlation with experimental findings was achieved by optimizing the heat transfer coefficient between the polymer and the mould, while using a multiscale mesh with a sufficient number of mesh elements. Optimal heat transfer coefficients between 10 000 $W/m^2{\cdot}K$ to 55 000 $W/m^2{\cdot}K$ were found for the different combinations of polymer and mould materials, which resulted in an accuracy of the simulated microneedle replication fidelity between 94.5 % to 97.0 %.

1. INTRODUCTION

Polymer products with micro surface features are increasingly used in multiple applications and industries such as microfluidics (Attia et al., 2009; Faraji Rad et al., 2017; Zhang et al., 2018), optics (Christiansen et al., 2014; Hopmann et al., 2015; Kalima et al., 2007; Loaldi et al., 2018), biomimetics (Huovinen et al., 2012; Iturri et al., 2015; Yamaguchi et al., 2015), and medical devices (Gornik, 2004; Padeste et al., 2011; Rytka et al., 2015). Microneedles are an example of microfeatures found in medical applications, which are often produced in polymers due to their excellent biocompatibility, biodegradability, and low material and production cost. These microneedles are used to pierce the skin, in order to deliver medical solutions or to extract human fluids from a body for sampling applications. Over the years, various types of microneedles have been developed, most often arranged in an array, having various shapes and lengths ranging from 25 to 2500 µm (Juster et al., 2019). Recently we developed a novel mass production method to produce solid (Evens et al., 2020) and hollow microneedle arrays (Evens et al., 2021b) using polymer injection moulding. Very sharp tipped microneedle cavities can be laser ablated in various mould materials and the cavity geometry can be adapted by changing laser scanning parameters as illustrated in (Evens, et al., 2021a).

Currently, extensive injection moulding experiments are needed to investigate the changes in the microneedle replication fidelity that result from variations in (i) the geometry of the macroscopic part, (ii) the shape, size and location of the microfeatures, (iii) the injection moulding processing parameters, (iv) the polymer properties, and (v) the mould material. These costly and time consuming experiments would be drastically reduced if sufficiently accurate injection moulding simulations can be made. Besides reducing the development time, numerical simulations would allow us to gain a better understanding of the underlying filling mechanisms for microfeatures.

Multiple commercially available computer-aided injection moulding simulation tools exist, such as, Moldex3D, Autodesk Moldflow, Sigmasoft, Simpoe-Mold, Cadmould, and Rem3D. These software packages describe the anisothermal, compressible, and viscous flow of molten polymers using Navier–Stokes equations, taking into account the conservation of mass, linear momentum, and energy (Kamal et al., 2009). Besides the Navier-Stokes equations, additional boundary conditions that describe the polymer flow are added to the system. The double domain Tait equation describes the pressure, volume, temperature (PVT) relationship, while the Cross-WLF (Cross–Williams–Landel–Ferry) model defines the velocity-dependent viscosity behaviour (Williams et al., 1955).

Injection moulding simulations are mostly used to predict the filling, warpage, formation of weld lines, etc. of macroscopic polymer products, yet some researchers have also addressed the filling of microfeatures. Kim & Turng (2006) were amongst the earliest to use a two-step macro-micro filling approach for the filling analysis of a part with a micro-surface feature. First, a filling analysis was performed at the macro-scale geometry of the part. Afterwards, a micro-level filling analysis on the micro-size geometry was performed, where the boundary conditions from the macro-level analysis were used as input data. A few years later, Lin & Young (2009) constructed a simplified model by assuming that most of the filling takes place during the packing phase. The model showed reasonable correlations with replication trials, yet the assumption that most of the filling takes place during the packing phase is not valid in all cases. Choi & Kim (2011) implemented both wall slip and surface tension in a multi-scale flow simulation, using Moldflow Autodesk and Comsol. They observed that a slip model was necessary for channels with a diameter less than 10 μm, and that the capillary effect was only noticeable in the submicron range. Birkar et al. (2016) utilized filling simulations with a multiscale mesh to provide insights on the spacing between micro surface features. They demonstrated that the spacing significantly affects the replication fidelity due to variations in the local packing pressure. Very recently, Loaldi et al. (2020) presented four case studies in which integrated multi-scale micro injection moulding simulations were employed as a digital process optimization tool. In one of the cases, the replication fidelity of microfeatures on a macroscopic part was predicted with a high accuracy of 91 %.

During an injection moulding cycle, the polymer undergoes a complex thermal process where it is heated to its processing temperature and afterwards injected into the mould cavity where it cools down and solidifies. Throughout this process, the heat transfer between the mould surface and polymer melt has a significant influence on the filling and cooling behaviour, which can in turn affect the component form, surface properties, internal morphology, residual stresses and physical properties (Babenko et al., 2018). This heat transfer is governed by the thermal contact conductance (TCC) or the heat transfer coefficient (HTC), being the term used in commercial software products. The HTC is affected by the area of the contacting surfaces, the temperature of the polymer and mould, the applied pressure and the surface topography (Babenko et al., 2018). The HTC at the interface of two surfaces in contact is given by (Madhusudana, 1996):

$$HTC = \frac{q}{T_h - T_c} \tag{1}$$

where q is the heat flux, T_h is the temperature at the 'hot' interface side and T_c is the temperature at the 'cold' interface side. A number of researchers have studied the heat transfer at polymer/metal interfaces through steady state experiments using an axial flow apparatus as described in (Narh & Sridhar, 2000). In this apparatus, a polymer sample is placed between two steel surfaces having a temperature gradient of 10 °C. Once a steady state was achieved, the heat flux was determined using thermocouples and the corresponding HTC was calculated. Using such apparatus, a range of varying HTC values was reported, being 250 W/m²·K and 1659 W/m²·K in the work of Marotta & Fletcher (1995), 15 000 W/m²·K and 25 000 W/m²·K in the work of Narh & Sridhar (1997) and around 7000 W/m²·K in the work of Dawson et al. (2008). However, these values were obtained using solid polymers, low pressures and constant thermal gradients, which is contradictory to the conditions in an injection moulding process.

Throughout the years, various researchers have adapted the default heat transfer coefficient in commercial simulations, in order to improve the correlation between simulations and experiments. For example, Nguyen-Chung et al. (2008) investigated the effect of the heat transfer coefficient on the injection pressure and filling degree of a micro spiral, and showed that a good correlation between Moldflow simulations and injection moulding could only be achieved by using a HTC of 15 000 W/m²·K and 25 000 W/m²·K. Tofteberg & Andreassen (2010) on the other hand, used a HTC of 30 000 W/m²·K in Moldflow and Ansys, to predict the filling of 2D optical gratings made of cyclic olefin copolymer (COP) with a 3 µm period. Zhang et al. (2019) assessed the replication fidelity of micro features on a microfluidic chip, while taking into account the heat transfer coefficient, venting, wall slip and the no-flow temperature. The heat transfer coefficient was varied from 1000 to 50 000 W/m²·K and the best prediction was found at a HTC of 30 000 W/m²·K. Xu et al. (2005) proposed a variable heat transfer coefficient within microchannels depending on the change in viscosity when the polymer is cooled down. They found that the variable heat transfer coefficient provided much better results than the conventional constant heat transfer coefficient. Babenko et al. (2018) also found that an increased HTC, compared to the default value, improved the accuracy of the simulated replication fidelity of microfeatures and suggested a HTC in the range of 7000 to 8000 W/m²·K for polypropylene and polystyrene. Rytka et al. (2016a) simulated the polymer melt flow into micro- and nano-features and compared the results to injection moulding trials. They adjusted the transition temperatures in the simulations with experimentally determined no-flow temperatures using melt flow index measurements and varied the heat transfer coefficient. They concluded that the heat transfer coefficient needed to be increased compared to appropriate values for macroscopic injection moulding simulations to correctly represent interfacial polymer/mould effects. Moreover, to confirm the necessity of a high HTC, they conducted heat transfer simulations using Comsol Multiphysics.

Largely all of the literature dealing with the simulation of microfeatures, investigated only one thermoplastic, one mould material and a fixed set of injection moulding conditions. In this study, we use Moldex3D to simulate the replication fidelity of polymer microneedles on a macroscopic plate and compare the results to injection moulding experiments. We investigate the simulated results for (i) two polymers, being polypropylene and polycarbonate, (ii) different locations of the microneedles on the macroscopic polymer part, (iii) different injection moulding parameters, and (iv) different mould materials being a tool steel, a copper alloy and an aluminium alloy. Moreover, the effect of the mesh size on the replication fidelity is investigated and an optimal heat transfer coefficient is determined for the different combinations of polymer and mould materials.

2. MATERIALS AND METHODS

2.1 *Thermoplastic polymers*

Two thermoplastic materials were used in this study, a polypropylene (PP, 578N, manufactured by SABIC) and a polycarbonate (PC, Lexan™ HPX8REU, manufactured by SABIC). The polypropylene material is a general purpose semi-crystalline homopolymer, which is easy to process and has a low cost. The polycarbonate material is a biocompatible amorphous grade, suitable for medical devices and pharmaceutical applications. Both materials have a high flowability as indicated by their very high melt flow index and are thus appropriate for filling small microfeatures. Table 1 reports the main characteristics for both thermoplastics.

Table 1 Main properties of the thermoplastics based on material datasheets and the Moldex3D 2020 material database.

	PP	PC
Density (kg/m^3)	905	1190
Melt flow index (g/10 min)	25 [230 °C/2.16 kg]	35 [300 °C/1.2 kg]
Elastic Modulus (MPa)	2100	2300
No-flow temperature (°C)	110	167

2.2 *Mould insert*

A low corrosion tool steel (Stavax, grade 1.2083), a high-strength aluminium zinc alloy (grade 3.4365) and a copper nickel alloy (grade AMPCOLOY 940) mould insert with 16 arrays of microneedle-cavities was manufactured in a previous study (Evens et al., 2021a). Each array has different microneedle dimensions and contains 9 microneedle cavities in a 3x3 setting. These cavities were created with a femtosecond laser ablation process, using a cross-hatching strategy (Evens et al., 2020). The dimensions of the ablated cavities were characterized using micro-computed tomography. The depth of the cavities varies between 720 µm and 2100 µm, with an aspect ratio ranging from 2.8 to 7.1; this geometry is shown in a previous study (Evens et al., 2021a). The thermal properties of the three mould materials are listed in Table 2.

The stationary side of the injection mould is equipped with a temperature sensor (Priamus, 4008B) and a piezoelectric pressure sensor (Priamus, 6001B), which allow for precise online measurement of the cavity temperature and pressure. Both sensors are located at a distance of 7 mm from the edge of the product, as illustrated in Figure 1.

Table 2 Thermal properties of the different mould materials based on material datasheets.

	Tool steel 1.2083	Aluminium 3.4365	Copper AMPCOLOY 940
Thermal conductivity at 100°C (W/m °C)	23.5	145	226
Specific heat capacity at 100°C (J/g °C)	0.48	0.95	0.38
Thermal diffusivity (mm²/s)	6.51	60.40	68.36

2.3 *Injection moulding product*

The injection moulded part selected for this study is a 50 mm x 60 mm x 1.5 mm flat plate, as shown in Figure 1. The polymer is injected through a hot runner which is located 2.3 mm from the edge of the product, indicated by a white dot. The microneedles are located in a 12 mm x 12 mm area being centred horizontally on the product and are vertically located 10 mm from the edge of the product.

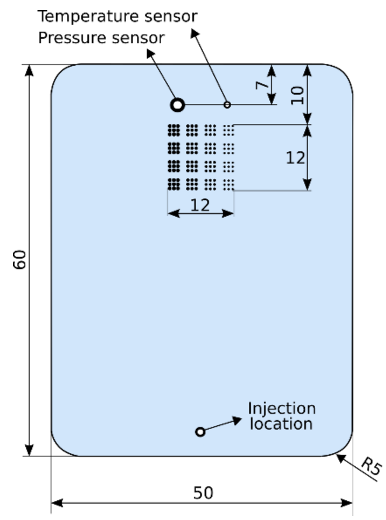

Figure 1 Illustration of the flat plate with all dimensions in mm, the thickness is 1.5 mm.

2.4 *Injection moulding experiments*

All injection moulding experiments were conducted on a Engel ES 200/35 HL hydraulic injection moulding machine with a maximum clamping force of 350 kN and a 25 mm horizontal screw. The machine is equipped with a hydraulic accumulator to increase the volumetric injection rate to a maximum of 149 cm^3/s. The mould temperature is controlled by a Wittmann Tempro D controller, with a maximum temperature of 180 °C.

The injection moulding parameters used in this study are given in Table 3. These values were determined experimentally to achieve a high replication fidelity. The injection temperature represents the adjustable barrel temperature and was set to the recommended upper limit of the material supplier. The mould temperature was set to a high value to delay the formation of the frozen layer during injection. The volumetric injection rate was set to a high value, to increase shear stresses and thus reduce the melt viscosity during injection. The implemented holding pressure was set to a value just below the occurrence of flash. For both polymers, the holding pressure time and cooling time were set to 4.5 and 6 seconds, respectively. This ensured that the gate was frozen at the end of the holding phase, and that good solidification of the product was achieved after the cooling phase. The switch-over point, being the position where the filling stage switches to the packing stage, was set to a screw position of 4.9 cm^3 for both materials. The total dosing volume was set to 10.8 cm^3 and 10.3 cm^3 for PC and PP respectively. The parts produced in the first 30 cycles were discarded in order to stabilize the process and the following 30 parts were collected for characterization.

The geometries of the replicated thermoplastic microneedles were assessed using a digital microscope (Keyence VH-S30) with a maximum magnification of X200. The system is connected to a VHX-500 F monitor with built-in measuring software. The microscope was calibrated using a stage micrometre (Olympus Tokyo, OBMM 1/100). 9 samples were injection moulded and to account for the injection moulding process repeatability, for each sample the first microneedle was measured on each array. Thus, on each injection moulded part, 16 different microneedles were measured. The average of these measurements along with a 95 % confidence interval, using the Student's t distribution was reported in the plotted results.

The total time needed to set-up the injection moulding machine, to mount the injection mould, to produce the injection moulded samples, and to measure the needle lengths of 9 samples was approximately 10 hours.

Table 3 Injection moulding process parameters for the two thermoplastic materials.

	PC	PP
Injection temperature (°C)	315	240
Volumetric injection rate (cm^3/s)	149	149
Holding pressure (MPa)	74.9	57.5
Mould temperature (°C)	115	80
Holding pressure time (s)	4.5	4.5
Cooling time (s)	6	6
Switch-over point (cm^3)	4.9	4.9
Dosing volume (cm^3)	10.8	10.2

3. INJECTION MOULDING SIMULATIONS SETTINGS

The commercial software package Moldex3D studio 2020 was used to simulate the injection moulding process. The polymer parts were meshed using Moldex3D designer with a boundary layer mesh to adequately represent the laminar flow of the melt. A three-layer prismatic mesh was generated inwards from the surface mesh and a tetrahedral mesh then filled up the remaining space, to ensure sufficient layers across the part thickness. Data of the thermoplastic materials such as viscosity, thermal properties and the pressure-volume-temperature relation (PVT) were obtained from the embedded Moldex3D software database. During preliminary simulations, it turned out that the cooling sequence, which takes into account the cooling circuit and mould material, did not affect the replication fidelity of the microfeatures. Thus, to decrease the computational time, only the filling sequence was conducted with a uniform mould temperature.

3.1 M*acroscopic flow*

It can be assumed that the macroscopic flow of the polymer is hardly affected by the microscopic surface features. However, the microscopic flow inside the microfeatures will be influenced by the macroscopic flow in terms of filling pressure, temperatures and flow front velocities. Thus, it is essential to compare the simulated macroscopic conditions to the experimental conditions. During injection moulding experiments using the tool steel insert and the in-mould sensors, we measured the cavity temperature and cavity pressure and compared them to the corresponding values obtained with Moldex3D flow simulations. For the simulation, the macroscopic part was meshed in 73000 elements and a “Filling & Packing” analysis was conducted using identical process conditions as the injection moulding experiments combined with the default setting of the heat transfer coefficient.

3.2 *Simulation parameters in Moldex3D*

Various simulation settings are important when simulating a macroscopic part with microscopic surface features. First of all, the injection moulding parameters should be identical to the ones used in the injection moulding experiments as they have a significant impact on the filling result. Thus, the holding pressure, melt temperature and mould temperature were set to the same values as in the experiments. The injection speed in Moldex3D was defined as a filling time, which was calculated using the volume of the part and the known volumetric injection rate. The calculated time corresponded to 0.06 seconds, which is in agreement with the experimental filling time of the injection moulding machine. Another important model parameter, is the heat transfer coefficient between the polymer and the mould. The HTC during the filling stage will be varied throughout the study, while the HTC during the packing and detached phase are set to 2500 W/m²·K and 1250 W/m²·K, i.e. the default values in Autodesk Moldflow. The detached phase represents the time after the packing phase, when the pressure on the mould wall equals zero until the end of the injection cycle. The last parameter that must be adapted from the default value is the criterion for stopping the calculation. This parameter is linked to a function which aims to decrease the computational time. As default, this value is set as 99.95 %, which means that if the product is filled for 99.95%, Moldex3D assumes that the part is completely filled, without a short shot and will end the simulation early to save computational time. In our case, the incomplete filling of the microfeatures is smaller than 0.05 % of the complete volume of the part, thus Moldex3D displays the part as completely filled. To overcome this problem, the criterion for stopping the calculation is changed into 99.9999 %, enabling the simulation of incomplete filled microfeatures. A summary of the adapted simulations parameters in Moldex3D can be found in Table 4.

Table 4 Default and adapted simulation parameters in Moldex3D.

Programme specific parameters	Default		Adapted	
	PP	PC	PP	PC
Holding pressure (MPa)	140	160	57.5	74.9
Melt temperature (°C)	240	305	240	315
Mould temperature (°C)	40	85	80	115
Filling time (s)	0.25	0.25	0.06	0.06
HTC during filling stage (W/m²·K)	Automatically determined		Variable	
HTC packing (W/m²·K)	Automatically determined		2500	
HTC detached (W/m²·K)	Automatically determined		1250	
Criterion for stopping calculation	99.95 %		99.9999 %	

3.3 *Mesh convergence study using multi-scale meshing*

An important parameter when conducting numerical simulations is the mesh size. Typically a finer mesh results in a more accurate solution, but as a downside requires an increased computation time. Therefore, a mesh convergence study is conducted to define a mesh size, having both a satisfactory solution and a computation time below 2 hours, using an Intel Core i7-9850H Processor. In this study, we varied the total number of mesh elements in the part from 430 000 to 4 900 000 elements in 6 steps. The first step, containing 430 000 elements, consisted out of a uniform mesh, containing roughly the same elements sizes, as illustrated in Figure 2 (a). However, the finite element mesh can also be split in different mesh densities, going from coarse to fine, also known as multi-scale meshing. A fine mesh is necessary within the microfeatures to achieve a precise simulation, while in the macroscopic part a coarse mesh is sufficient. In the transition zone between the coarse and fine elements, the element size needs to be changed gradually. Figure 2 (b) illustrates the multi-scale meshing strategy, corresponding to the 4 900 000 elements.

Using these 6 different sets of finite element meshes, we conducted filling simulations to determine the replication fidelity of the microneedle arrays for the tool steel insert. The height of the simulated microneedles were measured using a built-in measuring tool. For each simulation, the first microneedle on each array was measured, which is the same microneedle as the one measured experimentally. The height of the simulated microneedles were then compared to the average height of the injection moulded needles. The injection moulding parameters used in the simulations were identical to the experiments and the heat transfer coefficient during the filling phase for both thermoplastics were set to values found in literature. For PP the value was set to 10 000 $W/m^2 \cdot K$ as Nguyen-Chung et al. (2008) found a good correlation between Moldflow simulations and injection moulding with PP for this value. For PC the HTC was set to 30 000 $W/m^2 \cdot K$ as Rytka et al. (2016a), Xu et al. (2005), and Tofteberg & Andreassen (2010) reported a good correlation for PMMA and COP, both being amorphous materials.

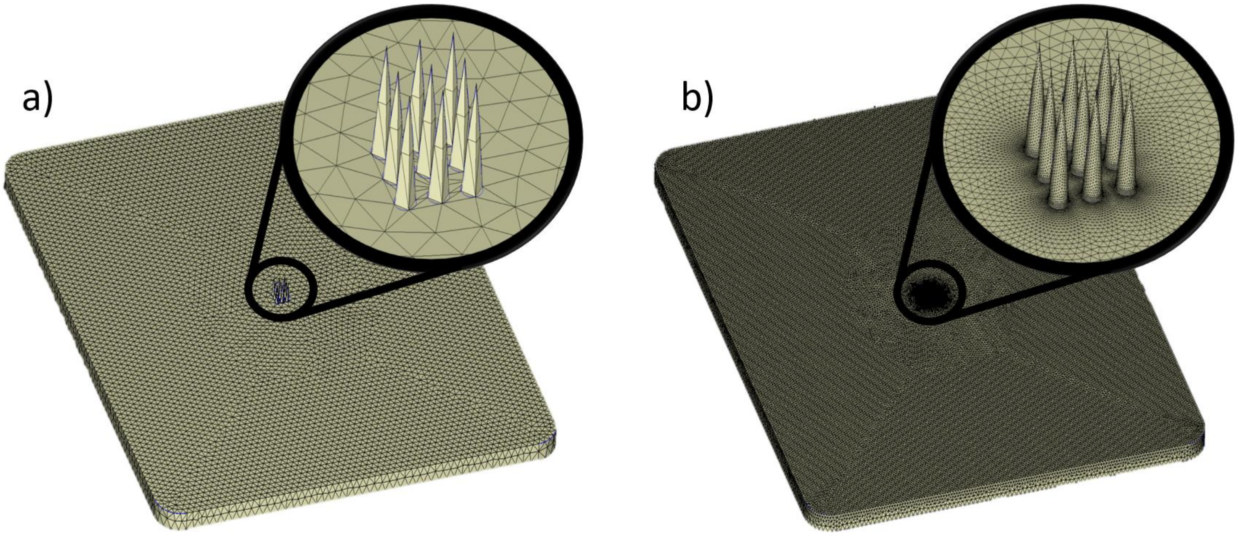

Figure 2 Illustration of (a) a uniform mesh corresponding to the 430 000 elements, and (b) multi-scale meshing corresponding to the 4 900 000 elements.

3.4 H*eat transfer coefficient*

As already indicated, the heat transfer coefficient, defining the heat transfer between the polymer melt and the surrounding mould material, is a very important parameter when conducting flow simulations with microscopic surface features. During the initial filling of the polymer melt inside the mould cavity, the temperature gradient between the mould and the melt is maximal, leading to a very high heat transfer between the polymer and the mould. As a result, the outer layer of the polymer cools down very fast, forming a solidified polymer skin layer near the mould surface. This frozen skin layer will act as an insulating barrier, leading to a substantial reduction in the heat transfer between the mould and the remaining molten core (Rytka et al., 2015). Thus, ideally in an injection moulding process the HTC should not be represented by a constant value, but by a variable in time as indicated by Sridhar et al. (1999,2000), Park & Kim (2019) and Rytka et al. (2016a). In the current commercially available simulations, it is only possible to specify a variable HTC coefficient in time for midplane or dual domain solvers in Autodesk Moldflow. In all other cases and software packages, it is only possible to set a constant value for the HTC throughout the whole filling simulation. In fact, the default HTC in Autodesk Moldflow 3D analysis is a constant value of 5000 $W/m^2 \cdot K$ for the filling stage. This moderate value of the HTC is a good assumption for macroscopic mould filling, as the melt contact with the mould surface is less important compared the bulk of the polymer. However, when filling microscopic cavities, an increased HTC during the initial contact is essential for the filling behaviour (Rytka et al., 2016a). In

Moldex3D, the default HTC is an automatically determined value, based on the selected materials and process conditions. The value of this automatically determined HTC is, however, not visible to the user. We determined a heat transfer coefficient, having the best correspondence with the experimentally determined replication fidelity, both for PP and PC in combination with the tool steel insert. This was done by varying the HTC from 5000 $W/m^2 \cdot K$ to 40000 $W/m^2 \cdot K$ and calculating the average absolute deviation between the simulated replication fidelity and the experimentally determined replication fidelity. Additionally, for both polymers we also performed a flow simulation using Moldex3D's default automatically determined HTC.

3.5 R*eplication fidelity in function of the location of the microfeatures*

From literature, it is known that the location of microfeatures on the macroscopic part will affect the replication fidelity. Microfeatures located near the gate will start to fill during the initial injection stage, while microfeatures located near the end of flow path will be filled during the end of the injection stage. This difference in timing causes the polymer melt to have a different temperature, pressure and viscosity during the filling of the microcavities, thus resulting in a different filling behaviour.

We validated the simulated replication fidelity in function of the location of the microfeatures on the macroscopic part by drawing comparisons with the injection moulding experiments. Two identical 3x3 microneedle cavities with an individual depths of 1730 μm were placed at two different locations on the macroscopic part. One array was placed at a distance of 2.3 mm from the injection location, while the other array was placed at 46.5 mm from the injection location, as depicted in Figure 3. 9 samples were injection moulded and to account for the injection moulding process repeatability, the first microneedle was measured for both arrays on each sample. The average of these 9 measurements along with a 95 % confidence interval, using the Student's t distribution was reported in the plotted results. The optimally determined HTC values determined in section 4.3 were used for both polymers.

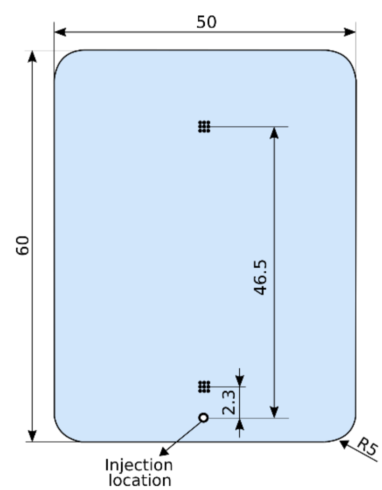

Figure 3 Illustration of the macroscopic part with two identical microneedle cavities, positioned at different distances from the injection location. All represented dimensions are in mm and the part thickness is 1.5 mm.

3.6 R*eplication fidelity in function of the injection moulding parameters*

The replication fidelity of microfeatures is greatly affected by the selected injection moulding process parameters, in particular the melt temperature, mould temperature, volumetric injection rate and the holding pressure (Tosello, 2018). The mould temperature is known in literature to be the most important parameter when it comes to replicating microfeatures (Attia et al., 2009; Baruffi et al., 2019; Tosello, 2018). This parameter determines how fast the frozen skin layer is formed, which hinders the filling of the microfeatures. A higher mould temperature delays the formation of the frozen skin layer and ensures that the polymer can still be deformed during the packing phase. Thus, a higher mould temperature results in a higher replication fidelity. The replication fidelity is also improved with a higher melt temperature, as it decreases the melt viscosity (Packianather et al., 2015). Furthermore, a high volumetric injection rate reduces the injection time and prevents premature freezing of the polymer. Besides, high injection velocities promote shear heating, decreasing the melt viscosity locally and therefore improve the replication fidelity (Tosello, 2018). The last parameter is the holding pressure. This parameter primarily compensates the volumetric shrinkage of the polymer and as such, preserves the replicated geometries during the filling stage. Besides, the holding pressure can also further improve the replication fidelity, at least if the initially filled layer can still be deformed. However, this is only possible if the temperature of the skin layer is still higher than the no-flow temperature and the holding pressure is sufficiently high (Baruffi et al., 2019; Zhang et al., 2018).

As the injection moulding parameters are of prime importance for the replication fidelity, we also compared the simulated and experimental replication fidelity for another set of injection moulding parameters. These adapted process conditions were set to a lower value compared to the elevated process conditions defined in section 2.4 and are illustrated in Table 5. 9 samples were injection moulded and to account for the injection moulding process repeatability, for each sample the first microneedle was measured on each array. The average of these 9 measurements along with a 95 % confidence interval, using the Student's t distribution was reported in the plotted results. The optimal HTC values determined in section 4.3 were used for both polymers.

Table 5 Adapted injection moulding process parameters for the two thermoplastic materials.

	PC	PP
Injection temperature (°C)	300	210
Volumetric injection rate (cm^3/s)	50	50
Holding pressure (MPa)	64.9	47.5
Mould temperature (°C)	85	40

3.7 R*eplication fidelity in function of the mould material*

The replication fidelity of the microfeatures is also influenced by the selected mould material, as illustrated by (Vera et al., 2018), Rytka et al. (2016b), Lucchetta et al. (2012) and Evens et al. (2021a). Therefore, we also determined the HTC, having the best correspondence with the experimentally determined replication fidelity, for the aluminium alloy and copper alloy in combination with PP and PC, using the same methodology as described in section 3.4 for tool steel. The aluminium alloy is typically used for low production series or prototype moulds and the copper alloy is preferred for its very high thermal conductivity which shortens the cooling phase. These mould materials exhibit different thermal properties, thus the previously determined optimal HTC values with the tool steel mould are not relevant anymore.

4. RESULTS AND DISCUSSION

4.1 M*acroscopic flow*

Figure 4 and Figure 5 illustrate the comparison between the simulated and experimental mould cavity pressure and temperature as a function of time for polypropylene and polycarbonate, respectively. The experimental curves, obtained using the in-mould sensors, show the average obtained pressure and temperature profile (n = 3) and the shaded area corresponds to the 95 % confidence interval. For polypropylene, the deviation between the simulation and the average absolute experimental pressure and temperature was 1.6 MPa and 9.3 °C, respectively. Similar results are found for polycarbonate, yet for the experimental pressure curve there is still a residual pressure inside the cavity, not predicted by the simulation. This residual pressure could be the result of the low shrinkage of the polycarbonate grade. For polycarbonate, the deviation between the simulation and the average absolute experimental pressure and temperature was 4.1 MPa and 12.2 °C, respectively. Overall, we can conclude that the simulated and experimentally determined mould cavity pressure is in good agreement for PP, while for PC the residual pressure inside the mould cavity was not predicted accurately. For the mould cavity temperature, it can be observed that there is a larger deviation between the experimental and simulated data, compared to the cavity pressure data. This indicates that there is still some room for improvements within the simulations.

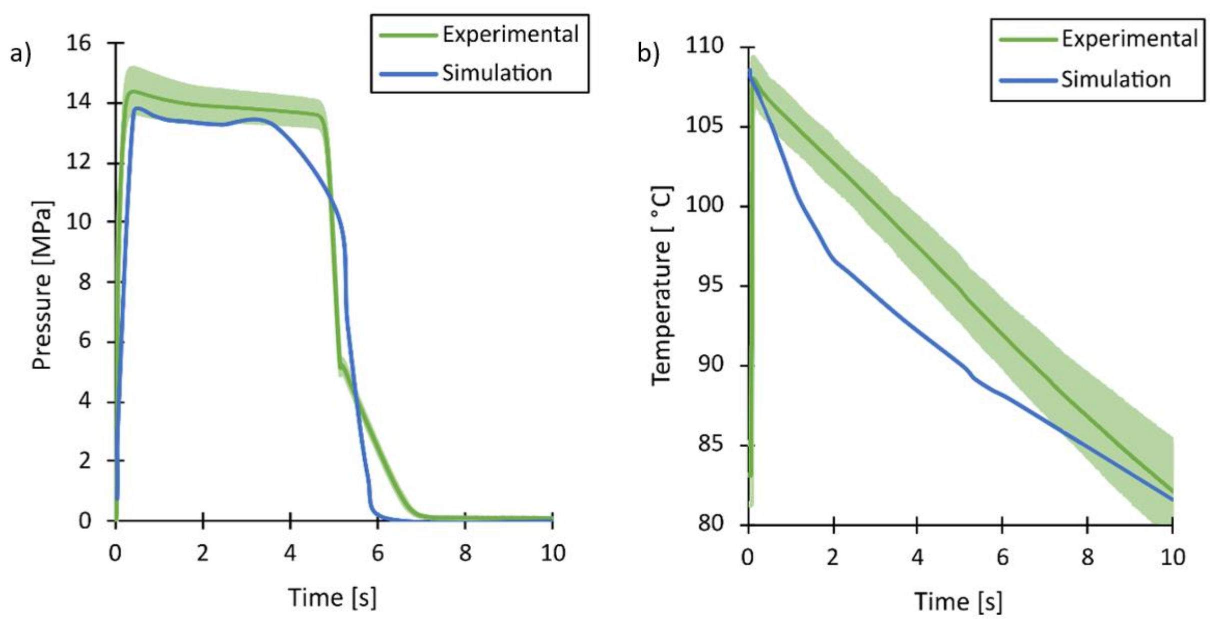

Figure 4 Comparison between the simulated and experimental mould cavity (a) pressure and (b) temperature in function of time for polypropylene. The experimental curve shows the average obtained

pressure and temperature profile (n = 3) and the shaded area corresponds to the 95 % confidence interval.

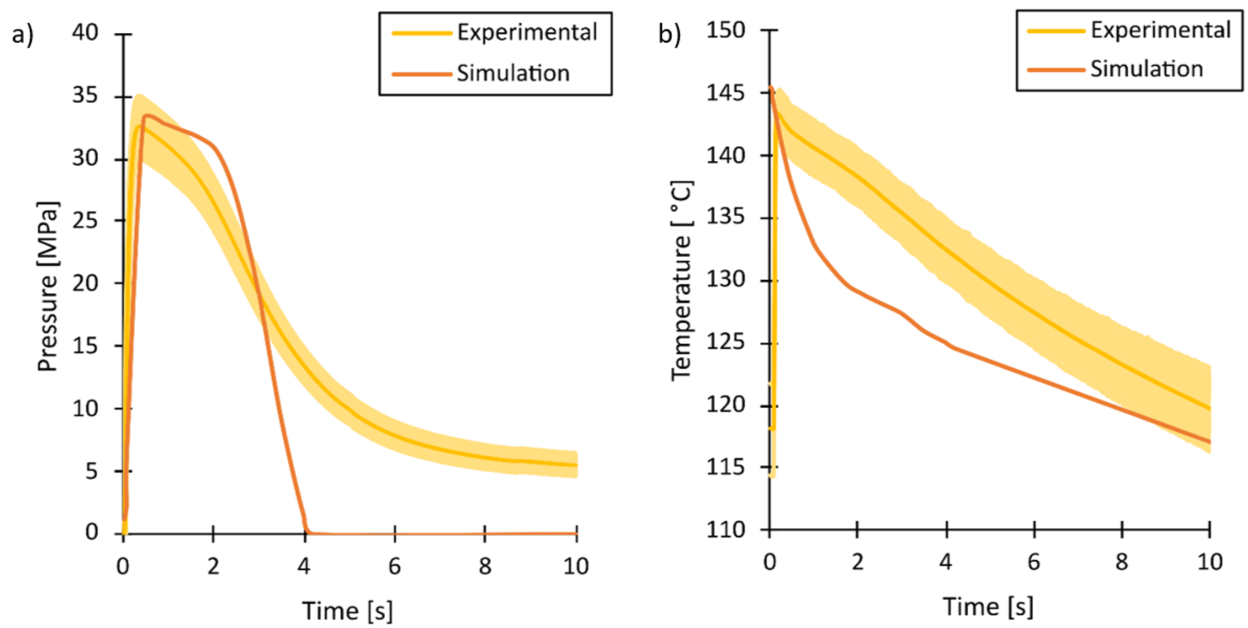

Figure 5 Comparison between the simulated and experimental mould cavity (a) pressure and (b) temperature in function of time for polycarbonate. The experimental curve shows the average obtained pressure and temperature profile (n = 3) and the shaded area corresponds to the 95 % confidence interval.

4.2 *Mesh convergence study*

The average absolute deviation between the simulated and experimental replication fidelity of the microneedles in function of the number of mesh elements for PP and PC is shown in Figure 6. It is observed that there is a high average absolute deviation at a low number of mesh elements, indicating a bad correspondence to the injection moulded experiments. However, with an increase of the number of mesh elements, the deviation in the replication fidelity in height between the simulations and experiments drastically decreases from ± 20 % to ± 4 %, for both thermoplastics. In addition, it is clear that the result converges with an increasing number of mesh elements and an accurate result is already found around 2.4 million mesh elements. Thus, in further simulations, the finite element mesh with 2.4 million mesh elements was used, as it results in a satisfactory solution with a computational time lower than 2 hours.

The time needed to predict the simulated replication fidelity of one sample with 16 microneedle arrays for one set of injection moulding parameters and one material combination corresponds to a maximum of 2 hours. In contrast, the time needed to determine the experimental replication fidelity of one sample with 16 microneedles arrays corresponds to approximately 10 hours. Thus, conducting an injection moulding simulation to predict the microneedle replication fidelity is at least 5 times faster compared to the experimental approach.

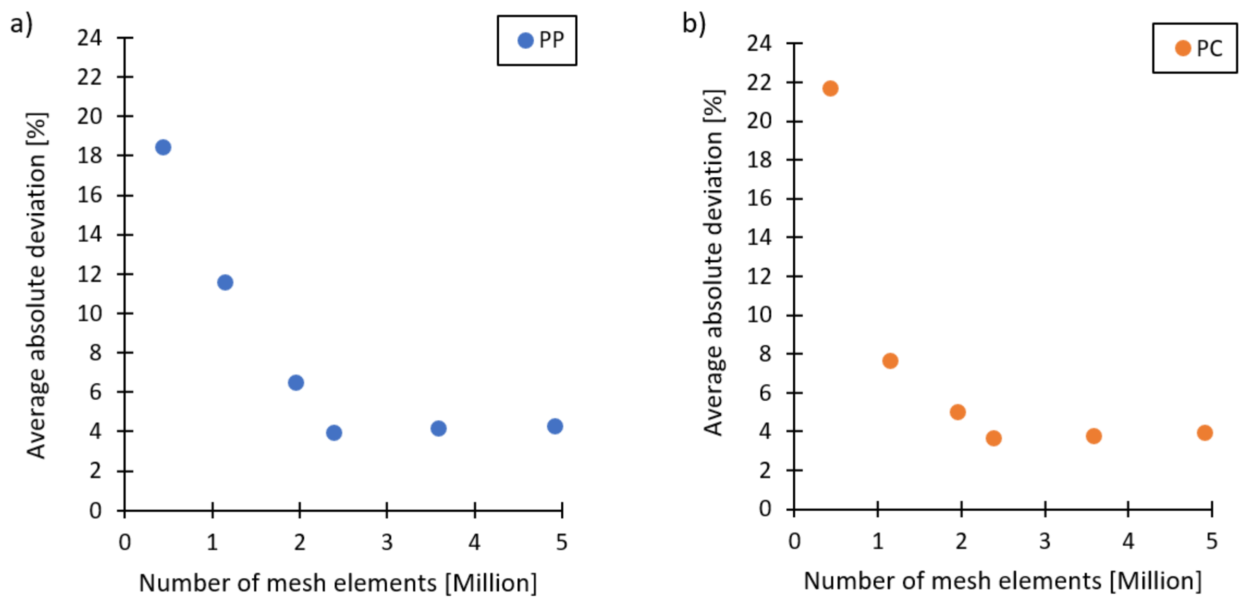

Figure 6 The average absolute deviation between the simulated and experimental replication fidelity of the microneedles in function of the number of mesh elements for (a) polypropylene and (b) polycarbonate.

4.3 Effect of the h*eat transfer coefficient*

The average absolute deviation between the simulated and experimental replication fidelity of the microneedles in function of the varied HTC for PP and PC is depicted in Figure 7. The red dotted lines correspond to the average absolute deviation when using the automatically determined HTC in Moldex3D. It is observed that the average absolute deviation between the simulated and experimental replication fidelity is clearly affected by the HTC value. At a low HTC, the simulated microneedles are overfilled compared to the experiments, indicated by a large deviation between the simulated and experimental replication fidelity. When the HTC is increased, the filling of the microneedles decreases and a minimum deviation is found. Further increasing the HTC results in a faster solidification of the simulated needles, causing the needles to be underfilled compared to the experiments. Thus, the deviation between the experimental and simulated replication fidelity starts increasing again. For PP the minimum deviation is found at a HTC of 10 000 W/m²·K, while for PC it is obtained at 30 000 W/m²·K. Both values correspond well to optimal HTC values found in literature , being 10 000 W/m²·K for PP [23] and 30 000 W/m²·K for PMMA and COP [24,28,29]. The difference in the optimal HTC value between the two thermoplastic polymers is due to the fact that these materials have different thermal properties, such the thermal conductivity, no-flow temperature, and heat capacity which affect the heat transfer between the thermoplastic and the mould material. A surprisingly low average absolute deviation is found between the simulations and experiments at the optimal HTC values of only 4.0 % and 3.7 % for PP and PC, respectively. Thus, the accuracy of the simulated replication fidelity corresponds to 96 % and 96.3 %. Besides, when using the default automatically determined HTC, the deviation between simulation and experiments are still acceptable, being 5.1 % and 7.2 % for PP and PC, respectively.

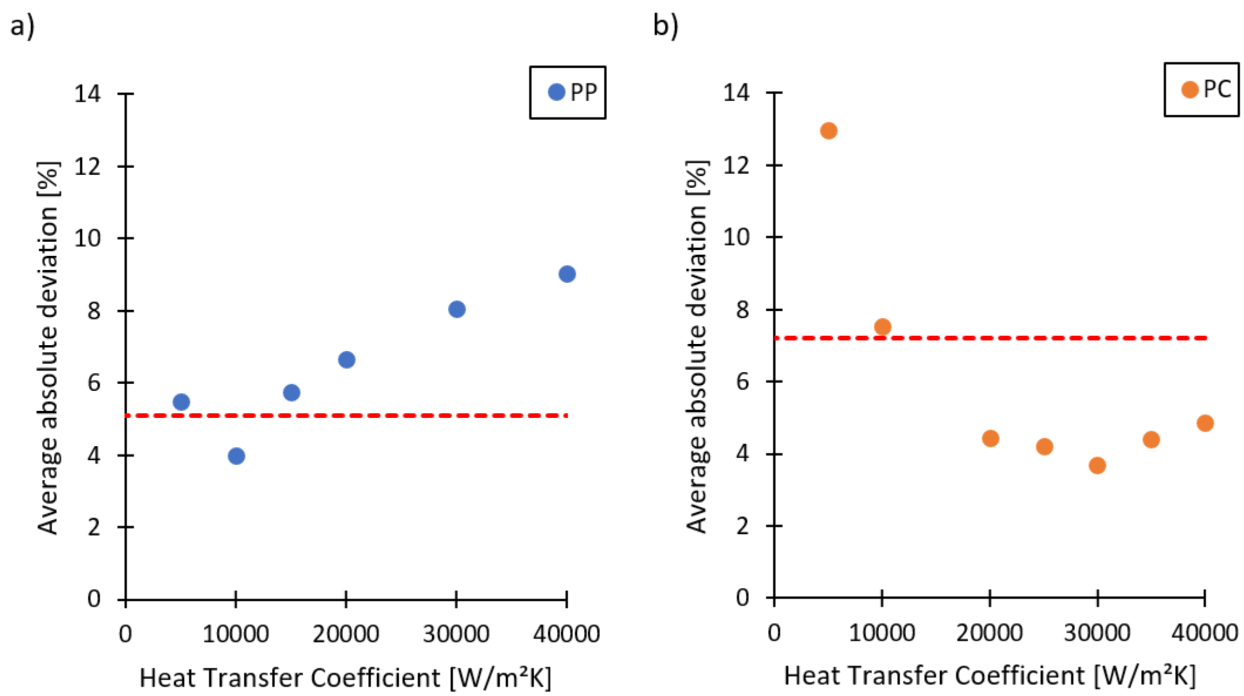

Figure 7 The average absolute deviation between the simulated and experimental replication fidelity of the microneedles in function of the varied HTC for (a) polypropylene and (b) polycarbonate. The red dotted lines correspond to the average absolute deviation when using the automatically determined HTC in Moldex3D.

Figure 8 shows the experimental and simulated replication in height of the 16 different microneedle arrays, in function of the aspect ratio of the microneedle cavity. The optimally determined HTC was used for both polymers, being 10 000 W/m²·K and 30 000 W/m²·K for PP and PC, respectively. A very good correlation between the experimental and simulated replication in height is observed both for PP and PC being 4.0 % and 3.7 %, respectively. Besides, a clear linear relationship between the replication in height and the aspect ratio of the corresponding microneedle cavities is found. This relationship is caused by two phenomena, being an increased hesitation effect with higher aspect ratio micro-cavities and an increased heat transfer due to the increased surface area to volume ratio, as previously discussed in (Evens et al., 2021a). Besides, it can be observed that the replication fidelity for the PP grade is higher compared to the PC grade, as the replication in height at an aspect ratio of 7 is approximately 40% for PC and only 15% for PP. This difference in replication is possibly caused by four factors, being linear shrinkage, interfacial wetting behaviour, creep deformation behaviour and melt viscosity as further discussed in (Evens et al., 2021a).

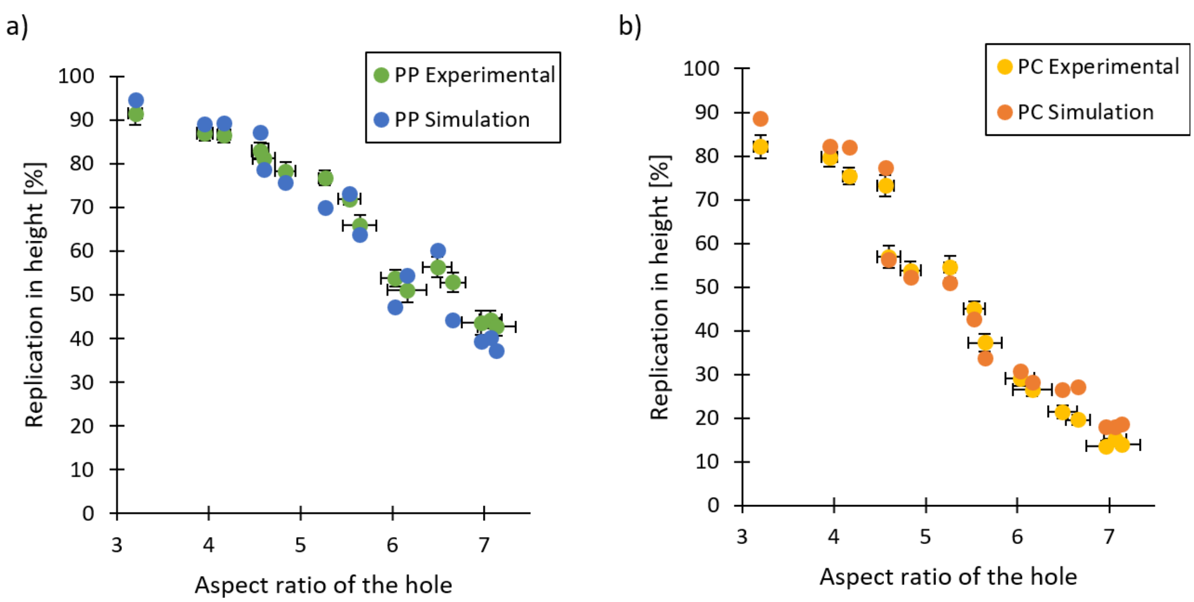

Figure 8 The experimental and simulated replication in height of the 16 different microneedle arrays, in function of the aspect ratio of the micro hole for (a) polypropylene with a HTC of 10000 W/m²·K and (b) polycarbonate with a HTC of 30000 W/m²·K. The vertical error bars represent the combined 95 % confidence interval of the hole depth and the replicated microneedle; the horizontal error bars represent the combined 95 % confidence interval of the hole depth and the hole diameter.

4.4 R*eplication fidelity in function of the location of the microfeatures*

Figure 9 illustrates the replication in height of the microneedles located close to the gate and far from the gate for PP and PC. Again, it can be seen that there is only a small deviation between the simulated replication in height and the corresponding experimentally determined height, for both the array located close to the gate and far from the gate. An average absolute deviation between the simulations and experiments of 5.9 % and 6.5 % was found for PP and PC, respectively. Thus, a good correspondence between the simulated replication fidelity and the experimentally determined replication fidelity is also found for a different location of the microfeatures on the macroscopic part.

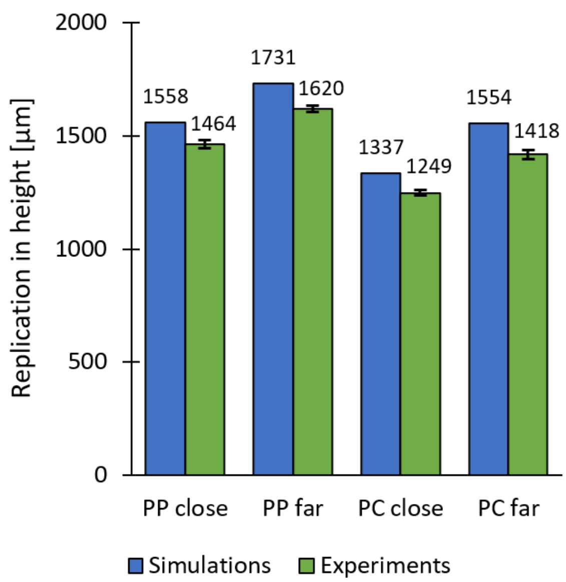

Figure 9 Difference in replication in height between the microneedles close to the gate and far from the gate for polypropylene and polycarbonate. The error bars represent the 95 % confidence interval.

A significant difference in the replication in height is observed between the microneedles located close to the gate and located far from the gate. The difference between the two locations is, as already indicated, a result of a different temperature, pressure and viscosity of the polymer melt during the filling of the two microneedle arrays. In our case, the microneedle array located far from the gate has a higher replication fidelity compared to the array located close to the gate. This result contradicts Lucchetta et al. (2014) who found a better replication fidelity for microfeatures closer to the gate.

However, the microfeatures investigated in their study are much smaller, being micro grooves with a width of 3 µm and an aspect ratio of 5. In their study, the microfeatures are solely filled during the initial filling stage, as the polymer immediately starts solidifying when coming in contact with the colder mould. Therefore, the area on the product with the highest pressure during the initial injection phase is located close to the gate and results in the best replication fidelity.

To explain the different filling behaviour observed in our case, we generated a XY cross-section of the part, enabling the visualisation of the temperature and pressure gradient throughout the width and thickness of the microneedle as illustrated in Figure 10 (a). The microneedles located close to the gate are almost completely filled during the initial filling stage as shown in Figure 10 (b) and Figure 10 (c). However, the melt rapidly starts cooling down from the moment of the initial contact with the mould. Consequently, at the moment when the cavity is completely filled and the cavity pressure is maximal, the temperature of the melt has already decreased far below the no-flow temperature and thus the microneedle is unable to be further filled. The initial filling of the microneedles located far from the gate is delayed due to increased flow length illustrated in Figure 10 (b) and Figure 10 (c). However, the temperature of the melt during the filling of the microneedles is still very high due to the characteristic fountain flow found for injection moulding. Only shortly after the melt reaches the microneedles far from the gate, the macroscopic part is completely filled and the pressure reaches a maximum, illustrated in Figure 10 (d) and Figure 10 (e). At that moment, the temperature within the needles located far from the gate is still above the no-flow temperature and thus ensures the needles to be further filled.

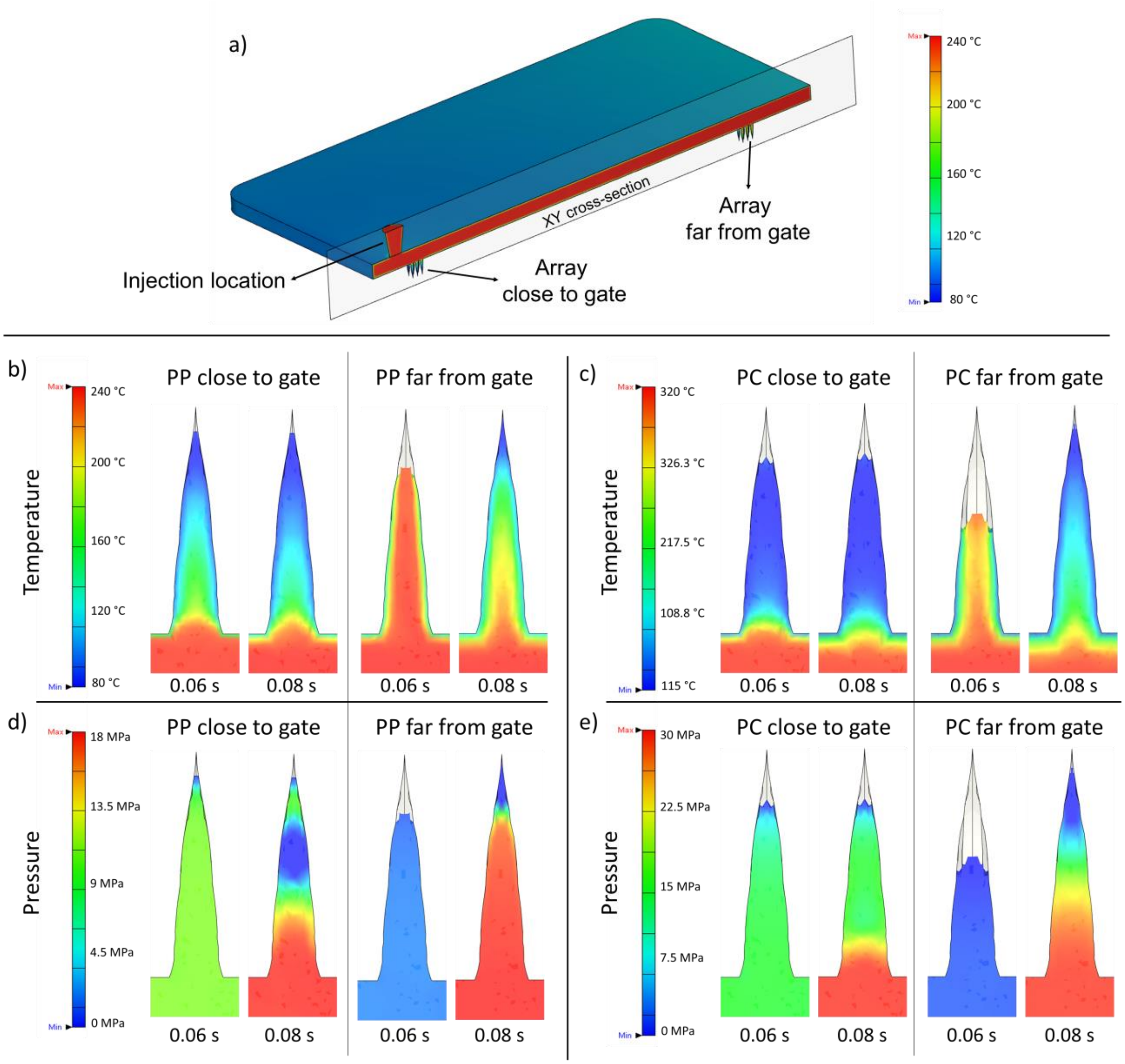

Figure 10 (a) Illustration of the XY cross-section of the PP part; cross-sections with time dependent filling and temperature progress of the microneedles close and far from the gate for (b) PP and (c) PC; cross-sections with time dependent filling and pressure progress of the microneedles close and far from the gate for (d) PP and (e) PC.

4.5 R*eplication fidelity in function of the injection moulding parameters*

Figure 11 illustrates the experimental and simulated replication in height of the microneedle arrays created with the adapted injection moulding parameters, in function of the aspect ratio of the micro hole, for PP and PC. As expected, the adapted lower injection moulding parameters illustrated in Table 5 resulted as a lower replication fidelity, compared to the replication fidelity created with the elevated injection moulding conditions, as described in section 4.3. Besides, when comparing the simulated and experimentally determined replication fidelity, it can be perceived that the results are in very good agreement. In fact, the average absolute deviation between the simulated and experimental replication fidelity of the 16 different arrays of 9 microneedles corresponds to 4.3 % and 4.4 % for PP and PC, respectively. Thus, a good correspondence between the simulation and experiments is also found when using different injection moulding parameters.

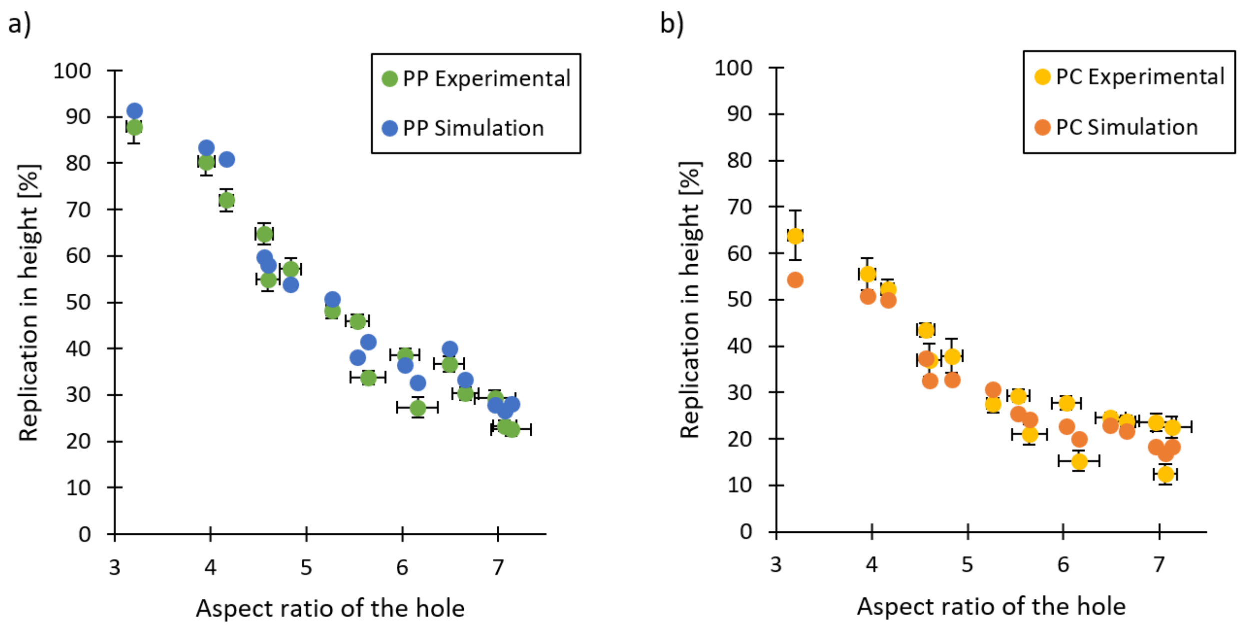

Figure 11 The experimental and simulated replication in height of the 16 different microneedle arrays created with the adapted injection moulding parameters, in function of the aspect ratio of the micro hole, for (a) polypropylene with a HTC of 10000 $W/m^2 \cdot K$ and (b) polycarbonate with a HTC of 30000 $W/m^2 \cdot K$. The vertical error bars represent the combined 95 % confidence interval of the hole depth and the replicated microneedle; the horizontal error bars represent the combined 95 % confidence interval of the hole depth and the hole diameter.

4.6 R*eplication fidelity in function of the mould material*

Figure 12 and Figure 13 depict the average absolute deviation between the simulated and experimental replication fidelity of the microneedles in function of the varied HTC for both polymers, in combination with the aluminium alloy and the copper alloy, respectively. Once again, the same trend is observed that with an increasing HTC, the deviation between the simulation and experiments decreases to a minimum, followed by an increase when the HTC is further increased. For the aluminium alloy, a minimal deviation of 3.0 % is found at a HTC of 25 000 $W/m^2{\cdot}K$ for PP, while for PC a minimal deviation of 5.5 % was observed at a HTC of 55 000 $W/m^2{\cdot}K$. For the copper alloy, a minimum deviation of 4.7 % is found for PP at 10 000 $W/m^2{\cdot}K$ and for PC a minimum of 3.3 % is found at 35 000 $W/m^2{\cdot}K$. Thus, also here a high simulation accuracy between 94.5 % to 97.0 % is found by varying the HTC value. For the aluminium and copper alloy, higher absolute average deviations are found when using the automatically HTC by Moldex3D. The highest deviation is observed for PC in combination with aluminium being 16.3 %, which indicates that this automatically determined HTC does not always result in a reliable solution.

Different optimal heat transfer coefficients are found for the three mould materials, as summarised in Table 6. The highest optimal HTC value for both polymers is found for the aluminium alloy insert, while the HTC values for tool steel and copper alloy insert are almost identical. One would assume that the highest thermal diffusivity would correspond to the highest heat transfer coefficient as demonstrated by Lucchetta et al. (2012). However, copper alloy having the highest thermal diffusivity, has a similar HTC value compared to tool steel. Thus, no clear correlation is found between the optimal HTC values and the thermal diffusivity (indicated in Table 2). However, there is a correlation between the HTC values and the experimentally determined replication fidelity for the different mould materials. In our previous study, it was shown that the replication fidelity of the microneedles with tool steel and copper alloy were comparable, while the replication fidelity with the aluminium alloy was significantly lower (Evens et al., 2021a). This was explained by the fact that the replication fidelity was not only influenced by the thermal properties of the mould material, but also by the wetting properties between the molten polymer and the mould surface. Tool steel exhibited the best thermal properties, being of a low thermal diffusivity which delayed the formation of the frozen layer, but it was combined with bad wetting properties. Copper alloy on the other hand had the best wetting property, combined with a high thermal diffusivity. The aluminium alloy however, had both bad thermal and wetting properties, which resulted in the lowest replication fidelity. Thus, if different mould materials are used, the heat transfer coefficient should be adapted to compensate both the thermal and the wetting properties.

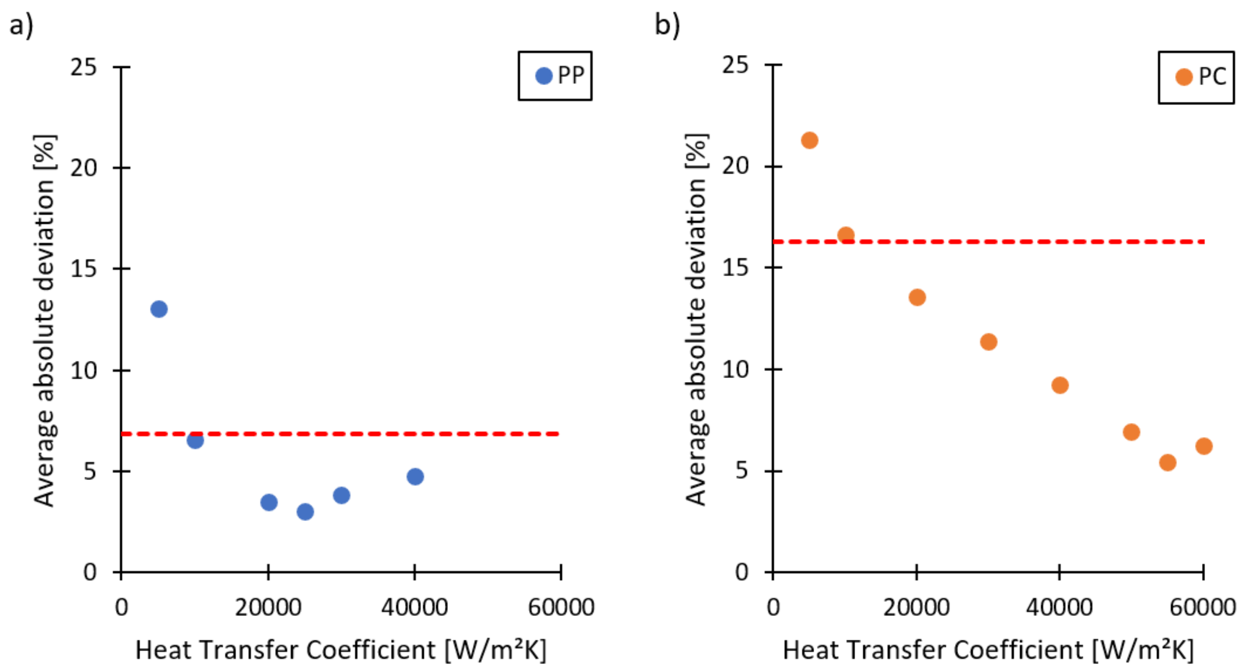

Figure 12 The average absolute deviation between the simulated and experimental replication fidelity of the microneedles created with the aluminium alloy, in function of the varied HTC for (a) polypropylene and (b) polycarbonate. The red dotted lines correspond to the average absolute deviation when using the automatically determined HTC in Moldex3D.

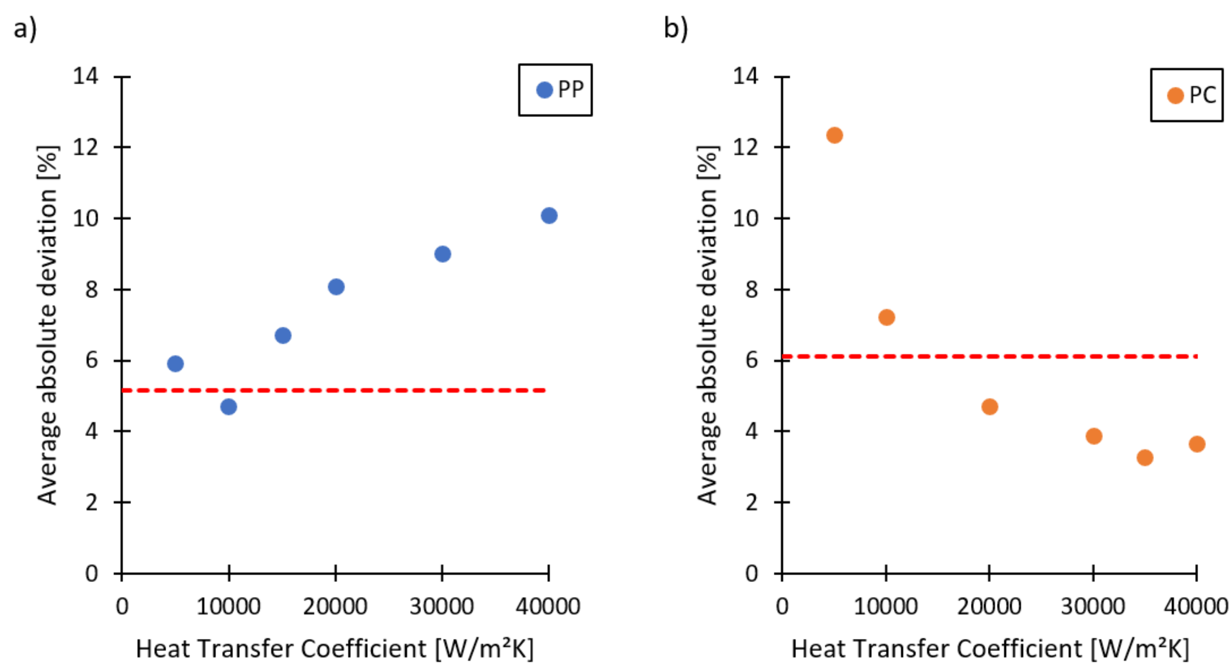

Figure 13 The average absolute deviation between the simulated and experimental replication fidelity of the microneedles created with the copper alloy, in function of the varied HTC for (a) polypropylene and (b) polycarbonate. The red dotted lines correspond to the average absolute deviation when using the automatically determined HTC in Moldex3D.

Table 6 Heat transfer coefficients, corresponding to a minimal average absolute deviation between the simulated and experimentally determined replication fidelity, for the PP and PC in combination with the tool steel, the aluminium alloy and the copper alloy mould insert.

	PC	PP
Optimal HTC for tool steel (W/m²·K)	10 000	30 000
Optimal HTC for aluminium alloy (W/m²·K)	25 000	55 000
Optimal HTC for copper alloy (W/m²·K)	10 000	35 000

Figure 14 and Figure 15 represent the experimental and simulated replication in height of the different microneedle arrays, in function of the aspect ratio of the microneedle cavity created with the aluminium alloy and copper alloy, respectively. The optimally determined HTC value was used for the different mould materials. As already indicated by the average absolute deviation, a very good correlation is found between the experimentally determined and simulated replication in height for both mould materials and polymers. This indicates that a good correspondence between simulation and experiments for different mould and polymer materials is possible, when using an adequate HTC.

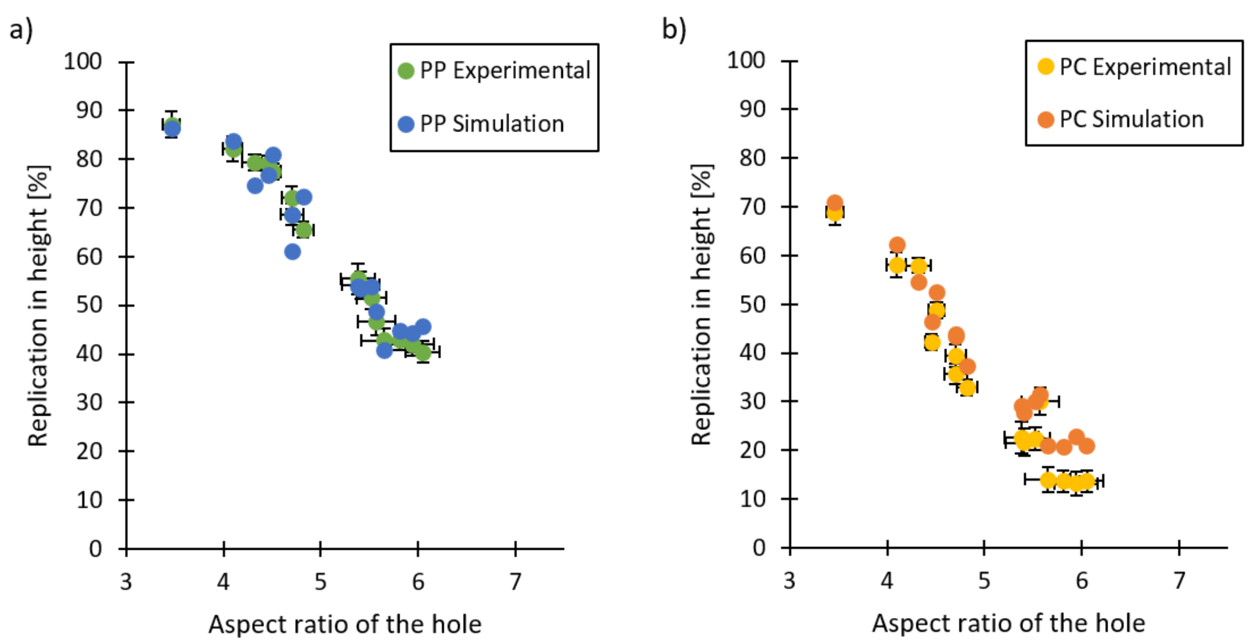

Figure 14 The experimental and simulated replication in height of the 16 different microneedle arrays created in the aluminium alloy, in function of the aspect ratio of the micro hole for (a) polypropylene

with a HTC of 25000 W/m²·K and (b) polycarbonate with a HTC of 55000 W/m²·K. The vertical error bars represent the combined 95 % confidence interval of the hole depth and the replicated microneedle; the horizontal error bars represent the combined 95 % confidence interval of the hole depth and the hole diameter.

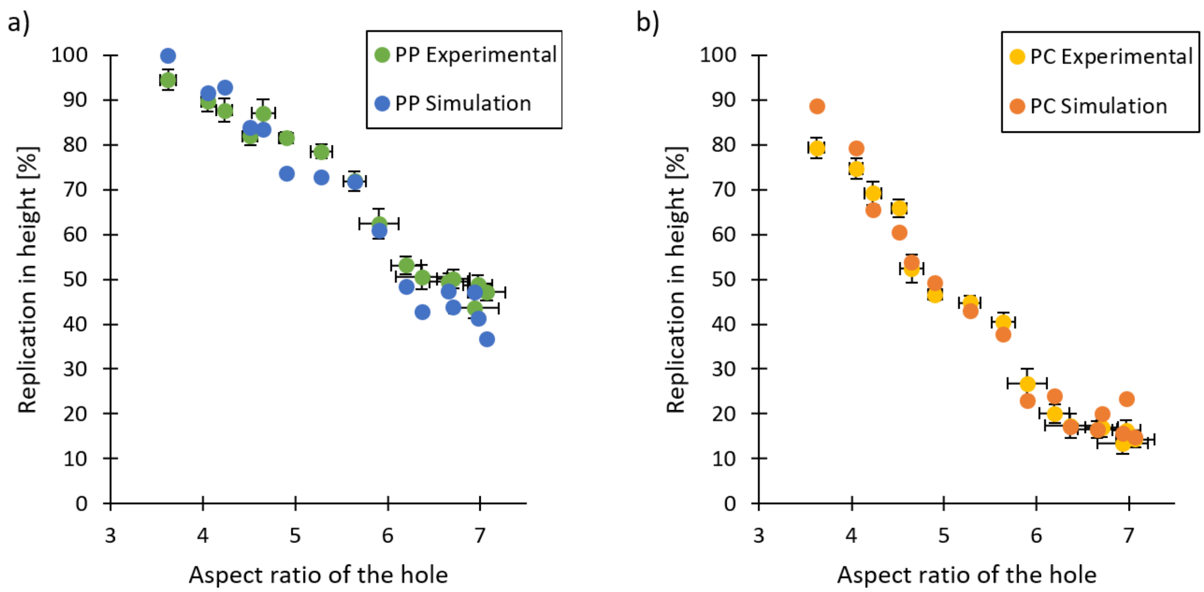

Figure 15 The experimental and simulated replication in height of the 16 different microneedle arrays created in the copper alloy, in function of the aspect ratio of the micro hole for (a) polypropylene with a HTC of 10000 W/m²·K and (b) polycarbonate with a HTC of 35000 W/m²·K. The vertical error bars represent the combined 95 % confidence interval of the hole depth and the replicated microneedle; the horizontal error bars represent the combined 95 % confidence interval of the hole depth and the hole diameter.

4 CONCLUSION

The present paper evaluated the simulated replication fidelity of polymer microneedles compared to injection moulding experiments. These simulations could greatly benefit the development of polymer microneedle arrays, as it would be possible to provide quick answers about optimal process parameters and mould materials to achieve a good replication fidelity for different microneedle sizes and geometries without the necessity of carrying out real injection moulding experiments. We validated the simulated replication fidelity for (i) polypropylene and polycarbonate, (ii) different locations of the microneedles on the macroscopic polymer part, (iii) different injection moulding parameters, and (iv) different mould materials being tool steel, copper alloy and aluminium alloy.

To reduce computational time, filling simulations were conducted without including cooling and warping sequences. Macroscale boundary conditions such as the cavity temperature and pressure were validated by comparing in-mould sensor measurements to simulated data-points. An accuracy of the simulated microneedle replication fidelity between 94.5 % to 97.0 % was achieved, when taking into account two key factors.

First, the mesh size is an important parameter to achieve accurate simulations. In fact, for macroscopic parts with micro surface features, it is recommended to use multi-scale meshing to achieve a finer mesh within the microfeatures, compared to the other regions of the macroscopic part. We conducted a mesh convergence study, to define a mesh size having both an acceptable solution and a computation time below 2 hours using an Intel Core i7-9850H Processor. It was found that the deviation between the simulations and experiments drastically decreases with an increase in mesh elements. Conducting an injection moulding simulation to predict the microneedle replication fidelity was at least 5 times faster compared to the experimental approach.

Second, the heat transfer coefficient is of prime importance when conducting filling simulations on microscopic features as it determines the formation of the frozen skin layer. We determined an optimal heat transfer coefficients for PP and PC in combination with the three different mould materials, by varying the HTC. Different optimal HTC values between 10 000 $W/m^2 \cdot K$ to 55 000 $W/m^2 \cdot K$ were found for the different mould and polymer combinations due to the differences in thermal and wetting properties. The minimum average deviation at the optimal HTC values was in all cases lower than the automatically determined HTC value by Moldex3D.

A difference in replication in height was observed between the microneedles located close to the gate and located far from the gate. The microneedles located far from the gate had a significantly higher replication fidelity compared to the array located close to the gate. This result was explained by the different temperature and pressure of the polymer melt, during the filling stage between the two different locations.

In summary, Moldex3D simulations can be used to accurately predict the filling behaviour of micro surface features on a macroscopic part for different micro-feature sizes and geometries, different injection moulding parameters, different polymers and different feature locations on the macroscopic part, while using an adequate HTC and mesh size.

FUNDING

This work was funded by the KU Leuven Interdisciplinary Network project IDN/20/011 - MIRACLE: Autonomous microfluidic patch for plasmid-based vaccine.

ACKNOWLEDGEMENTS

The authors would like to thank Olivier Malek from the company Sirris, department Precision Manufacturing (Belgium) for laser ablating the microneedle cavities in the mould inserts. We also thank the company SABIC for providing the thermoplastic injection moulding materials and the company SimpaTec for their support with the Moldex3D analyses.

REFERENCES

Attia, U. M., Marson, S., & Alcock, J. R., “Micro-injection moulding of polymer microfluidic devices,” Microfluid. Nanofluidics, 7(1), 1–28, (2009) DOI: 10.1007/s10404-009-0421-x

Babenko, M., Sweeney, J., Petkov, P., Lacan, F., Bigot, S., & Whiteside, B., “Evaluation of heat transfer at the cavity-polymer interface in microinjection moulding based on experimental and simulation study,” Appl. Therm. Eng., 130, 865–876, (2018) DOI: 10.1016/j.applthermaleng.2017.11.022

Baruffi, F., Gülçür, M., Calaon, M., Romano, J.-M., Penchev, P., Dimov, S., Whiteside, B., & Tosello, G., “Correlating nano-scale surface replication accuracy and cavity temperature in micro-injection moulding using in-line process control and high-speed thermal imaging,” J. Manuf. Process., 47(August), 367–381, (2019) DOI: 10.1016/j.jmapro.2019.08.017

Birkar, S., Mendible, G., Park, J.-G., Mead, J. L., Johnston, S. P., & Barry, C. M. F., “Effect of feature spacing when injection molding parts with microstructured surfaces,” Polym. Eng. Sci., 56(12), 1330–1338, (2016) DOI: 10.1002/pen.24164

Choi, S., & Kim, S. K., “Multi-scale filling simulation of micro-injection molding process,” J. Mech. Sci. Technol., 25(1), 117–124, (2011) DOI: 10.1007/s12206-010-1025-9

Christiansen, A. B., Clausen, J. S., Mortensen, N. A., & Kristensen, A., “Injection moulding antireflective nanostructures,” Microelectron. Eng., 121, 47–50, (2014) DOI: 10.1016/j.mee.2014.03.027

Dawson, A., Rides, M., Allen, C. R. G., & Urquhart, J. M., “Polymer-mould interface heat transfer coefficient measurements for polymer processing,” Polym. Test., 27(5), 555–565, (2008) DOI: 10.1016/j.polymertesting.2008.02.007

Evens, T., Malek, O., Castagne, S., Seveno, D., & Van Bael, A., “A novel method for producing solid polymer microneedles using laser ablated moulds in an injection moulding process,” Manuf. Lett., 24, 29–32, (2020) DOI: 10.1016/j.mfglet.2020.03.009

Evens, T., Malek, O., Castagne, S., Seveno, D., & Van Bael, A., “Controlling the geometry of laser ablated microneedle cavities in different mould materials and assessing the replication fidelity within polymer injection moulding,” J. Manuf. Process., 62(July 2020), 535–545, (2021) DOI:

10.1016/j.jmapro.2020.12.035

Evens, T., Van Hileghem, L., Dal Dosso, F., Lammertyn, J., Malek, O., Castagne, S., Seveno, D., & Van Bael, A., “Producing Hollow Polymer Microneedles Using Laser Ablated Molds in an Injection Molding Process,” J. Micro Nano-Manufacturing, 9(3), 1–9, (2021) DOI: 10.1115/1.4051456

Faraji Rad, Z., Nordon, R. E., Anthony, C. J., Bilston, L., Prewett, P. D., Arns, J.-Y., Arns, C. H., Zhang, L., & Davies, G. J., “High-fidelity replication of thermoplastic microneedles with open microfluidic channels,” Microsystems Nanoeng., 3(1), 17034, (2017) DOI: 10.1038/micronano.2017.34

Gornik, C., “Injection Moulding of Parts with Microstructured Surfaces for Medical Applications,” Macromol. Symp., 217(1), 365–374, (2004) DOI: 10.1002/masy.200451332

Hopmann, C., Weber, M., Schöngart, M., Schäfer, C., Bobzin, K., Bagcivan, N., Brögelmann, T., Theiß, S., Münstermann, T., & Steger, M., “Injection moulding of optical functional micro structures using laser structured, PVD-coated mould inserts,” AIP Conf. Proc., 1664, 110003, (2015) DOI: 10.1063/1.4918478

Huovinen, E., Hirvi, J., Suvanto, M., & Pakkanen, T. A., “Micro–Micro Hierarchy Replacing Micro–Nano Hierarchy: A Precisely Controlled Way To Produce Wear-Resistant Superhydrophobic Polymer Surfaces,” Langmuir, 28(41), 14747–14755, (2012) DOI: 10.1021/la303358h

Iturri, J., Xue, L., Kappl, M., García-Fernández, L., Barnes, W. J. P., Butt, H.-J., & del Campo, A., “Torrent Frog-Inspired Adhesives: Attachment to Flooded Surfaces,” Adv. Funct. Mater., 25(10), 1499–1505, (2015) DOI: 10.1002/adfm.201403751

Juster, H., van der Aar, B., & de Brouwer, H., “A review on microfabrication of thermoplastic polymer-based microneedle arrays,” Polym. Eng. Sci., 59(5), 877–890, (2019) DOI: 10.1002/pen.25078

Kalima, V., Pietarinen, J., Siitonen, S., Immonen, J., Suvanto, M., Kuittinen, M., Mönkkönen, K., & Pakkanen, T. T., “Transparent thermoplastics: Replication of diffractive optical elements using micro-injection molding,” Opt. Mater. (Amst)., 30(2), 285–291, (2007) DOI: 10.1016/j.optmat.2006.11.046

Kamal, M., Isayev, A., & Liu, S.-J., Injection molding technology and fundamentals 1st ed., Carl Hanser

Verlag, (2009)

Kim, S.-W., & Turng, L.-S., “Three-dimensional numerical simulation of injection molding filling of optical lens and multiscale geometry using finite element method,” Polym. Eng. Sci., 46(9), 1263–1274, (2006) DOI: 10.1002/pen.20585

Lin, H.-Y., & Young, W.-B., “Analysis of the filling capability to the microstructures in micro-injection molding,” Appl. Math. Model., 33(9), 3746–3755, (2009) DOI: 10.1016/j.apm.2008.12.012

Loaldi, D., Quagliotti, D., Calaon, M., Parenti, P., Annoni, M., & Tosello, G., “Manufacturing Signatures of Injection Molding and Injection Compression Molding for Micro-Structured Polymer Fresnel Lens Production,” Micromachines, 9(12), 653, (2018) DOI: 10.3390/mi9120653

Loaldi, D., Regi, F., Baruffi, F., Calaon, M., Quagliotti, D., Zhang, Y., & Tosello, G., “Experimental Validation of Injection Molding Simulations of 3D Microparts and Microstructured Components Using Virtual Design of Experiments and Multi-Scale Modeling,” Micromachines, 11(6), 614, (2020) DOI: 10.3390/mi11060614

Lucchetta, G., Ferraris, E., Tristo, G., & Reynaerts, D., “Influence of mould thermal properties on the replication of micro parts via injection moulding,” Procedia CIRP, 2(1), 113–117, (2012) DOI: 10.1016/j.procir.2012.05.051

Lucchetta, G., Sorgato, M., Carmignato, S., & Savio, E., “Investigating the technological limits of micro-injection molding in replicating high aspect ratio micro-structured surfaces,” CIRP Ann., 63(1), 521–524, (2014) DOI: 10.1016/j.cirp.2014.03.049

Madhusudana, C. V., “Thermal Contact Conductance,” In F. Ling, E. Gloyna, & W. Howard (Eds.), *Control*, Springer New York, (1996) DOI: 10.1007/978-1-4612-3978-9

Marotta, E. E., & Fletcher, L. S., “Thermal contact conductance of polymeric materials,” 33rd Aerosp. Sci. Meet. Exhib., 10(2), (1995) DOI: 10.2514/6.1995-421

Narh, K. A., & Sridhar, L., “Measurement and modeling of thermal contact resistance at a plastic metal interface,” ANTEC Conf. Proc., 2, 2273–2277, (1997)

Narh, K. A., & Sridhar, L., U.S. Pat. 6142662, New Jersey Institute of Technology, (2000) Nguyen-Chung, T., Jüttner, G., Pham, T., Mennig, G., & Gehde, M., “The importance of precise boundary conditions for the simulation of micro-injection molding,” J. Plast. Technol., 4(6), (2008)

Packianather, M., Griffiths, C., & Kadir, W., “Micro Injection Moulding Process Parameter Tuning,” Procedia CIRP, 33, 400–405, (2015) DOI: 10.1016/j.procir.2015.06.093

Padeste, C., Özçelik, H., Ziegler, J., Schleunitz, A., Bednarzik, M., Yücel, D., & Hasırcı, V., “Replication of high aspect ratio pillar array structures in biocompatible polymers for tissue engineering applications,” Microelectron. Eng., 88(8), 1836–1839, (2011) DOI: 10.1016/j.mee.2010.11.051

Park, E. M., & Kim, S. K., “Effects of Mold Heat Transfer Coefficient on Numerical Simulation of Injection Molding,” Trans. Korean Soc. Mech. Eng. - B, 43(3), 201–209, (2019) DOI: 10.3795/KSME-B.2019.43.3.201

Rytka, C., Kristiansen, P. M., & Neyer, A., “Iso- and variothermal injection compression moulding of polymer micro- and nanostructures for optical and medical applications,” J. Micromechanics Microengineering, 25(6), 065008, (2015) DOI: 10.1088/0960-1317/25/6/065008

Rytka, C., Lungershausen, J., Kristiansen, P. M., & Neyer, A., “3D filling simulation of micro- and nanostructures in comparison to iso- and variothermal injection moulding trials,” J. Micromechanics Microengineering, 26(6), 065018, (2016) DOI: 10.1088/0960-1317/26/6/065018

Rytka, C., Opara, N., Andersen, N. K., Kristiansen, P. M., & Neyer, A., “On The Role of Wetting, Structure Width, and Flow Characteristics in Polymer Replication on Micro- and Nanoscale,” Macromol. Mater. Eng., 301(5), 597–609, (2016) DOI: 10.1002/mame.201500350

Sridhar, L., & Narh, K. A., “Computer Simulation of the Effect of Thermal Contact Resistance on Cooling Time in Injection Molding,” Simulation, 73(3), 144–148, (1999) DOI: 10.1177/003754979907300301

Sridhar, L., Sedlak, B. M., & Narh, K. A., “Parametric Study of Heat Transfer in Injection Molding—Effect of Thermal Contact Resistance,” J. Manuf. Sci. Eng., 122(4), 698–705, (2000) DOI: 10.1115/1.1287348

Tofteberg, T. R., & Andreassen, E., “Multiscale Simulation of Injection Molding of Parts with Low Aspect

Ratio Microfeatures," Int. Polym. Process., 25(1), 63–74, (2010) DOI: 10.3139/217.2318

Tosello, G., "Micro Injection Molding," In G. Tosello (Ed.), *Micro Injection Moldin.*, Carl Hanser Verlag GmbH & Co. KG, (2018) DOI: 10.3139/9781569906545

Vera, J., Brulez, A.-C., Contraires, E., Larochette, M., Trannoy-Orban, N., Pignon, M., Mauclair, C., Valette, S., & Benayoun, S., "Factors influencing microinjection molding replication quality," J. Micromechanics Microengineering, 28(1), 015004, (2018) DOI: 10.1088/1361-6439/aa9a4e

Williams, M. L., Landel, R. F., & Ferry, J. D., "The Temperature Dependence of Relaxation Mechanisms in Amorphous Polymers and Other Glass-forming Liquids," J. Am. Chem. Soc., 77(14), 3701–3707, (1955) DOI: 10.1021/ja01619a008

Xu, G., Yu, L., Lee, L. J., & Koelling, K. W., "Experimental and numerical studies of injection molding with microfeatures," Polym. Eng. Sci., 45(6), 866–875, (2005) DOI: 10.1002/pen.20341

Yamaguchi, M., Sasaki, S., Suzuki, S., & Nakayama, Y., "Injection-molded plastic plate with hydrophobic surface by nanoperiodic structure applied in uniaxial direction," J. Adhes. Sci. Technol., 29(1), 24–35, (2015) DOI: 10.1080/01694243.2014.973158

Zhang, H., Fang, F., Gilchrist, M. D., & Zhang, N., "Filling of high aspect ratio micro features of a microfluidic flow cytometer chip using micro injection moulding," J. Micromechanics Microengineering, 28(7), 075005, (2018) DOI: 10.1088/1361-6439/aab7bf

Zhang, H., Fang, F., Gilchrist, M. D., & Zhang, N., "Precision replication of micro features using micro injection moulding: Process simulation and validation," Mater. Des., 177, 107829, (2019) DOI: 10.1016/j.matdes.2019.107829